J. Electrochem. Sci. Eng. **12(2)** (2022) 331-341; http://dx.doi.org/10.5599/jese.1237

Open Access : : ISSN 1847-9286

https://pub.iapchem.org/ojs/index.php/JESE

Original scientific paper

Sensitive determination of uric acid at layered zinc hydroxide-sodium dodecyl sulphate-propoxur nanocomposite

Mohamad Hafiz Ahmad Tajudin[1,2], Mohamad Syahrizal Ahmad[2,3,✉], Illyas Md Isa[2,3], Norhayati Hashim[2,3], Anwar Ul-Hamid[4], Mohamad Idris Saidin[2,3], Rahadian Zainul[5] and Suyanta M. Si[6]

[1]*Faculty of Applied Sciences, Universiti Teknologi MARA, Perak Branch, Tapah Campus, Tapah Road, 35400 Perak, Malaysia*

[2]*Department of Chemistry, Faculty of Science and Mathematics, Universiti Pendidikan Sultan Idris, 35900 Tanjong Malim, Perak, Malaysia*

[3]*Nanotechnology Research Centre, Faculty of Science and Mathematics, Universiti Pendidikan Sultan Idris, 35900 Tanjong Malim, Perak, Malaysia*

[4]*Center for Engineering Research, Research Institute, King Fahd University of Petroleum & Minerals, Dhahran 31261, Saudi Arabia*

[5]*Department of Chemistry, Faculty of Mathematics and Natural Science, Universitas Negeri Padang, West Sumatera 25171, Indonesia*

[6]*Department of Chemistry Education, Faculty of Mathematics and Natural Science, Yogyakarta State University, Indonesia*

Corresponding author: ✉ *syahrizal@fsmt.upsi.edu.my; Tel.: +60-196266485; Fax: +60-54506000*

Received: January 15, 2022; Accepted: February 15, 2022; Published: February 26, 2022

Abstract

An electrochemical chemical sensor for the determination of uric acid (UA) with high sensitivity and a wide working range was fabricated using the layered zinc hydroxide-sodium dodecyl sulphate-propoxur (LZH-SDS-PRO) nanocomposite, modified with multiwall carbon nanotubes (MWCNT). The introduction of LZH-SDS-PRO as a conducting matrix has enhanced the conductivity of MWCNT. The morphology of LZH-SDS-PRO/MWCNT was characterized by transmission electron microscopy (TEM) and scanning electron microscopy (SEM), while electrochemical behavior of UA and $K_3[Fe(CN)_6]$ at LZH-SDS-PRO/MWCNT paste electrode was studied by square wave and cyclic voltammetry, respectively. Under the optimized experimental conditions, the electrode established linear plot for UA concentrations 7.0 mol L^{-1} to 0.7 mmol L^{-1} (R^2 = 0.9920) and LOD was calculated to be 4.28 µmol L^{-1} (S/N = 3). The fabricated LZH-SDS-PRO/MWCNT electrode was successsfully applied to urine samples, exhibiting excellent stability and reproducibility, which made it worthwhile for analytical applications.

Keywords

Electrochemical sensor; pharmaceutical sensor; modified MWCNT; layered metal hydroxide; functional nanocomposite; square wave voltammetry

Introduction

2,6,8-trihydroxypurine, also known as uric acid (UA), is a fundamental electroactive molecule resulting from the metabolism of endogenous purine, which occurs inside the human body [1,2]. Biological responses such as inflammation, vasoconstriction, oxidative stress and endothelial dysfunction can be stimulated by UA. Identifying diseases such as gout, hyperuricemia, kidney stone, type-2 diabetes, renal impairment, and Lesch-Nyan syndrome can be done by quantifying the concentration level of UA in blood and urine [3,4].

Various high precision, accurate and robust methods have been developed for analytical purposes, such as chromatography, fluorescence, electrophoresis, chemiluminescence and spectrophotometry, but all these methods are energy-consuming, high-cost, time-consuming and need complex operating processes [5-11]. Since UA is highly electrochemically active compound, alternative electrochemical methods were developed and characterized by cost-effectiveness, fastness, simplicity and portability for quantitative analysis.

Different functional materials have been introduced in developing UA sensors to improve the electron transfer of UA at electrodes, such as Co(II)-based zeolitic imidazolate framework [12], platinum nanoparticles (PtNPs) [13,14], nano resin [15] and ferrocene derivative and core-shell magnetic nanoparticles [16].

Since the first discovery of carbon nanotubes (CNT) in 1991, various materials have been incorporated into them and attracted widespread attention in the field of electroanalysis [17]. The unique electrochemical properties of CNT in terms of large surface area, excellent electron transfer, fine structure and light-weight make them be good electrodes for various applications [18-20]. In recent studies, multi-walled carbon nanotubes (MWCNT) were more preferable than single-walled CNT (SWCNT) due to rapid electron transfer for different reactions and better conductivity [21]. Besides, metal layered hydroxides have also gained much attention in carbon paste electrode (CPE) fabrication, owing to their remarkable capability of anion exchange and also excellent physicochemical properties in terms of low toxicity, chemical inertness and high surface area [22]. In our previous work, abilities of layered zinc hydroxide-ferulate (LZH-F), layered zinc hydroxide-*L*-phenylalanate (LZH-LP) and layered zinc hydroxide-sodium dodecyl sulphate-isoprocarb (LZH-SDS-ISO) applied as modifiers with MWCNT were demonstrated for the determination of hydroquinone (HQ) [23], acetaminophen (PCM) [24] and dopamine (DOP) [25], respectively.

Propoxur or 2-isopropoxyphenyl-*N*-methylcarbamate, was introduced to the market in 1959 and widely used in the pest control industry. Intercalation of propoxur with layered zinc hydroxide produces a nanocomposite material that has good electron transfer ability and a large surface-to-volume ratio. It has also been reported that this material shows low toxicity, high thermal stability, biocompatibility and the potential for controlled release [26,27]. Based on the listed advantages, in this work, we are presenting for the first time LZH-SDS-PRO material as a mediator used to increase the electrocatalytic activity of the redox reaction important for the determination of UA.

Experimental

Chemicals and reagents

The uric acid stock solution was prepared by dissolving the appropriate amount of UA in 0.1 mol L^{-1} NaOH solution. Potassium acetate, chloride salts (Sigma-Aldrich, USA), paraffin oil, copper(II) sulphate, potassium nitrate, potassium iodide, phosphate buffer solution (PBS) (K_2HSO_4 and KH_2SO_4) (Merck, Germany), barium chloride, glucose, fructose, sucrose and MWCNT (Timesnano, China) were of analytical grade and used as received. Ultra-pure water was used during the work.

Apparatus

FESEM model SU8020 UHR (Hitachi, Japan) and FETEM model JEM2100F (Jeol, Japan) were used for the characterization of surface morphologies of LZH-SDS-PRO/MWCNT and MWCNT. Potentiostat/galvanostat model Ref 3000 (USA) was used for electrochemical impedance spectroscopy (EIS) measurements, while cyclic voltammetry (CV) and square wave voltammetry (SWV) were conducted using Potentiostat series-G750 (USA). Three-electrode system was used in this study, where LZH-SDS-PRO/MWCNT, a platinum wire and Ag/AgCl electrode MF-2052 (Bioanalytical syst, USA) with fiber junction, acted as the working electrode, counter electrode and reference electrode, respectively.

Preparation of LZH-SDS-PRO nanocomposite

LZH-SDS was prepared by the addition of 40 mL of 0.5 M of $Zn(NO_3)_2{\cdot}6H_2O$ and 1.0 M NaOH into a solution of 40 mL of 0.25 M SDS. The pH value was adjusted to 6.5. Then, the slurry was centrifugated and dried in an oven at 70 °C.

Intercalation of propoxur into the interlayer of LZH-SDS was done by an ion-exchange method. 0.5 g of LZH-SDS was dissociated in 0.001 M propoxur solution and kept under a magnetic stirrer for 3 hours. The slurry was then aged 24 hours in an oil bath at 70 °C. After that, the slurry was centrifuged and the white solid was dried in an oven [26].

Electrode preparation

LZH-SDS-PRO (5 mg), MWCNT (100 mg) and paraffin oil (3 drops) were mixed using mortar and pestle. The homogenized mixture was firmly packed into Teflon tubing (*i.d.* 2.0 mm and 3 cm long). To establish the electrical contact, one of the ends of the paste was connected to the copper wire, and the other end was smoothened using soft paper. The non-modified MWCNT electrode was prepared with the same method but without LZH-SDS-PRO added.

Measurement procedure

UA solutions present at desired concentrations in 0.1 mol L^{-1} PBS (pH 6.4) as the supporting electrolyte were used throughout the work to perform voltammetry unless otherwise stated. The UA solutions were deoxygenated with N_2 before measurements for about 15 minutes. SWV experiments of UA determination were performed between 100 mV to 500 mV, with a frequency of 150 Hz, pulse height of 60.0 mV and step increment of 6.0 mV. CVs taken between -300 to 800 mV at the scan rate of 100 mV s^{-1} were applied for electrochemical characterization of the fabricated electrode with $K_3[Fe(CN)_6]$ as a redox probe. For EIS measurements, the frequency range of 10 kHz to 0.1 Hz and amplitude of the alternating voltage of 5.0 mV were used. All experiments were conducted at the ambient temperature of 25 ± 1 ^oC.

Results and discussion

Surface morphology

The SEM image of LZH-SDS-PRO shown in Figure 1, resembles nanoflower-like particles with a thickness of approximately 1.5 – 3.0 µm. To confirm the formation of LZH-SDS-PRO nanocomposite, EDS analysis was carried out. Different areas were focused during the EDS measurement and the conforming peaks were observed. The LZH-SDS-PRO can be seen in the synthesized composite nanostructure in the EDS spectrum. In the spectrum A, the quantity of C, Zn and O (measured in wt.%) were 40.1, 29.4 and 22.6, respectively, while in spectrum B, the values were 50.3, 29.5 and 17.0 % for C, Zn and O, respectively.

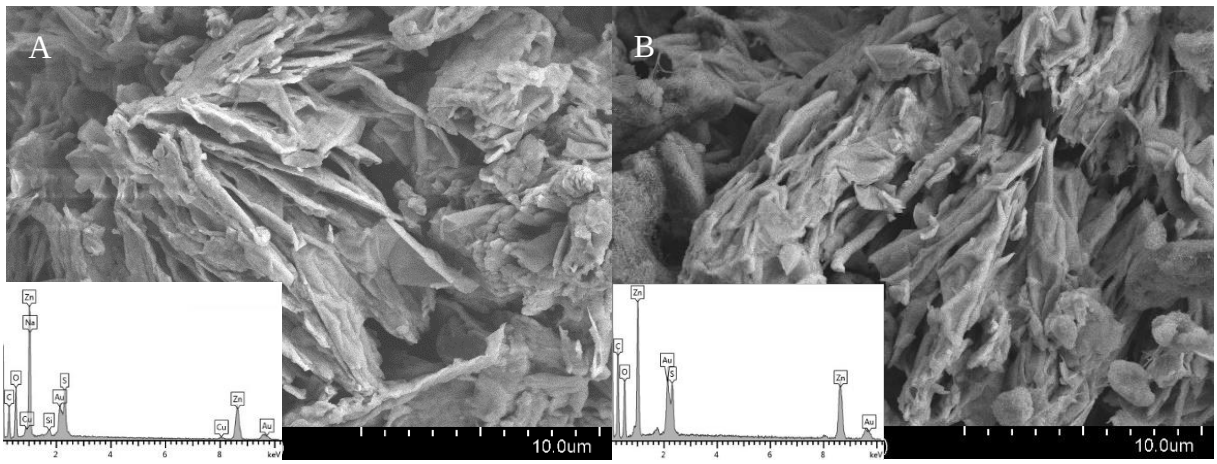

***Figure 1**. SEM image and EDS spectrum of (A) LZH-SDS-PRO and (B) LZH-SDS-PRO/MWCNT*

TEM analysis was performed to further investigate the morphology of the LZH-SDS-PRO composite. Figure 2 shows TEM images of the composite nanostructure at a low magnification where sharp edges and smooth surface of LZH-SDS-PRO (A) and carbon nanotubes strings (B) were observed, confirming the results from SEM images.

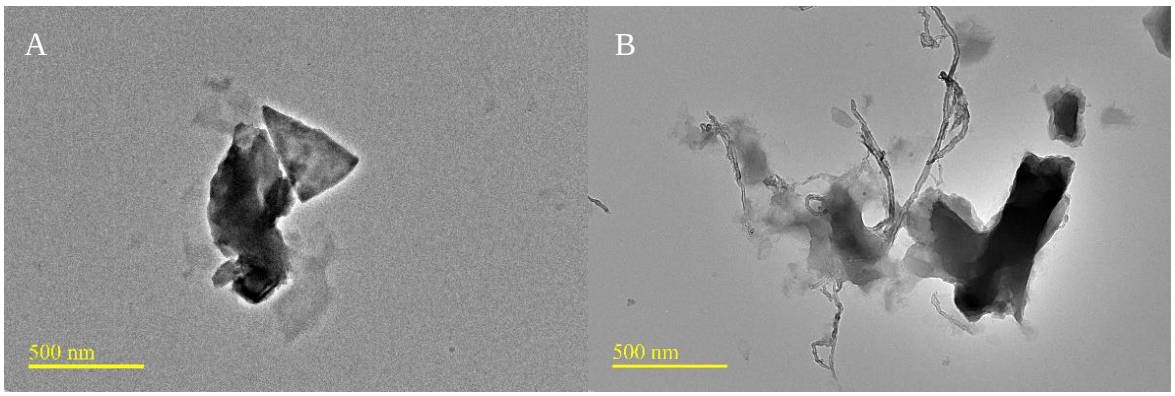

***Figure 2**. TEM image of (A) LZH-SDS-PRO and (B) LZH-SDS-PRO/MWCNT*

Electrochemical response of $K_3[Fe(CN)_6]$ at LZH-SDS-PRO/MWCNT paste electrode

Figure 3 shows CV voltammograms of 4.0 mmol L^{-1} $K_3[Fe(CN)_6]$ contained in 0.1 mol L^{-1} KCl at the LZH-SDS-PRO/MWCNT and unmodified MWCNT paste electrodes.

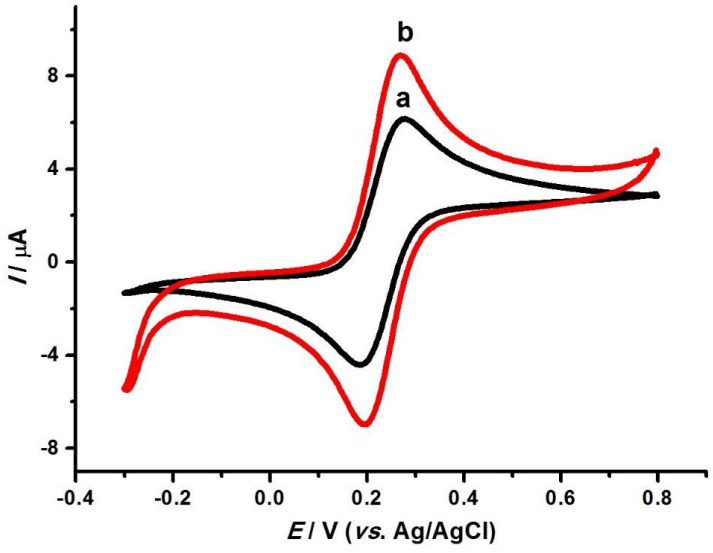

***Figure 3.** Cyclic voltammograms of (a) non-modified MWCNT and (b) LZH-SDS-PRO/MWCNT for 4.0 mmol L^{-1} $K_3[Fe(CN)_6]$ in 0.1 mol L^{-1} KCl, at scan rate 100 mV s^{-1}*

The LZH-SDS-PRO/MWCNT paste electrode showed redox peak current at I_{pa} = 8.743 µA, I_{pc} = 7.618 µA, and peak-to-peak separation (ΔE_p) = 71.6 mV. Meanwhile, redox peak current of the non-modified MWCNT paste electrode was I_{pa} = 5.854 µA, I_{pc} = 5.843 µA, and ΔE_p = 92.7 mV. It is evident from these findings that the introduction of LZH-SDS-PRO as an MWCNT modifier is responsible for improving electron transfer rate, electroactive surface area and the conductivity performance of the modified electrode.

The investigation of interfacial redox reaction kinetics of $[Fe(CN)_6]^{3-/4-}$ redox probe at LZH-SDS-PRO/ /MWCNT paste electrode was done by using the EIS method. The charge transfer resistance, R_{ct} values were estimated as diameters of semicircles appearing in high-frequency regions of Nyquist plots, where the diffusion process is represented by straight-line plots at lower frequencies [28]. In the inset of Figure 4, the Randles equivalent circuit used for fitting measured impedance spectra is presented. R_{ct} value for bare MWCNT paste electrode was 1.325 kΩ, while R_{ct} for LZH-SDS-PRO/ /MWCNT was 0.245 kΩ. It is clearly observed that LZH-SDS-PRO/MWCNT displayed lower charge transfer resistance within the interfacial layer, as suggested by more than five times smaller diameter of the semicircle.

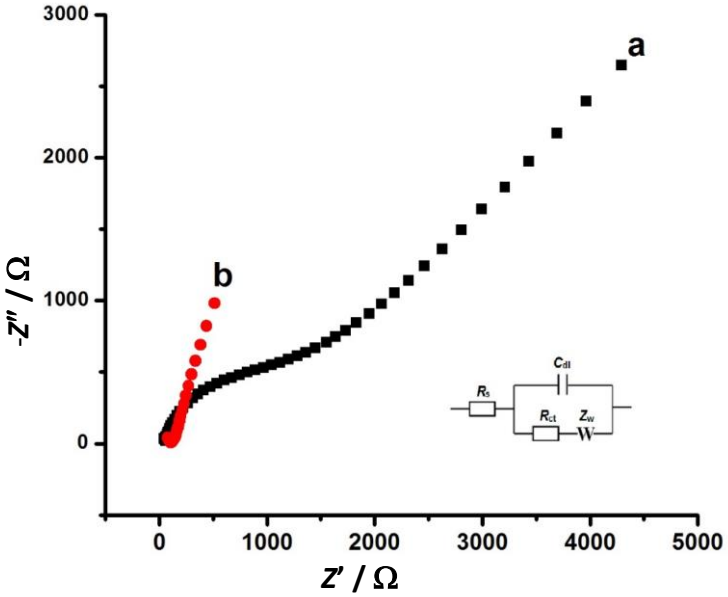

Figure 4. *Nyquist plots recorded in the solution of 4.0 mmol L^{-1} $K_3[Fe(CN)_6]$ in 0.1 mol L^{-1} KCl using (a) non-modified MWCNT, and (b) LZH-SDS-PRO/MWCNT paste electrode. Inset: Randles equivalent electrical circuit used for data fitting*

The apparent rate constant, k_{app} of the electron transfer on unmodified MWCNT and LZH-SDS--PRO/MWCNT paste electrode was 1.17×10^{-5} and 6.38×10^{-5} cm s^{-1}, respectively, which was calculated using the eq. (1):

$$k_{app} = RT/F^2 R_{ct} c \quad (1)$$

where T represents temperature, R is the gas constant, c is the concentration of $K_3[Fe(CN)_6]$ and F is Faraday's constant.

As a consequence of the high specific area and high conductivity, LZH-SDS-PRO/MWCNT electrode effectively promotes the electron transfer process.

The effect of scan rate (ν) change on the redox peak currents of 4.0 mmol L^{-1} $K_3[Fe(CN)_6]$ contained in 0.1 mol L^{-1} KCl at LZH-SDS-PRO/MWCNT paste electrode was also studied. As can be observed in Figure 5A, anodic and cathodic peak currents were progressively increased with increasing scan rate from 10 to 300 mV s^{-1}, while their E_p values shifted positively and negatively, respectively, suggesting kinetic limitation in the reaction [29]. In addition, there is also a straight-line relationship between peak current and scan rate (ν) with the linear regression equations, I_{pa} = 0.0635 ν + 3.9461 (R^2 = 0.9910) and I_{pc} = -0.0636 ν - 3.599 (R^2 = 0.9903) as shown in Figure 5B.

Besides that, the graph of peak currents versus square root of scan rate ($\nu^{1/2}$) was plotted in Figure 5C, showing a good linear relationship with the following linear equations: I_{pa} = 1.2679 $\nu^{1/2}$ - 1.1281 and I_{pc} = -1.2566 $\nu^{1/2}$ + 1.394. The correlation coefficients obtained were 0.9913 and 0.9927, respecttively. These results revealed that the redox reaction of $K_3[Fe(CN)_6]$ on LZH-SDS-PRO/MWCNT paste electrode is reversible, *i.e.* diffusion-controlled [30].

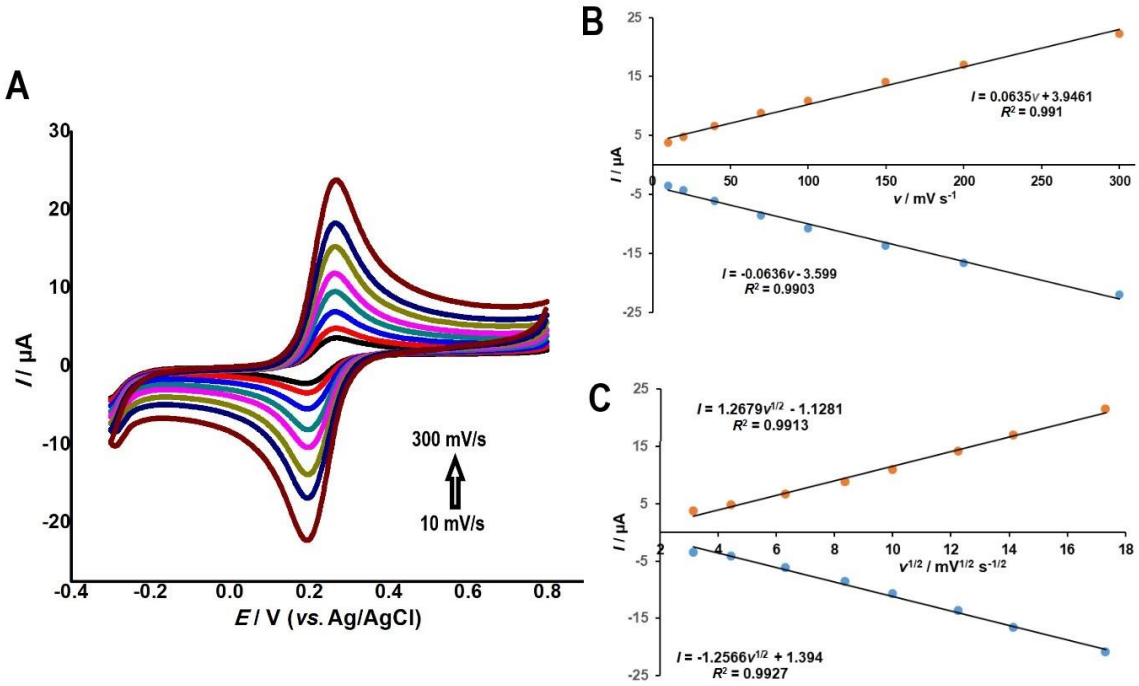

Figure 5. *(A) Cyclic voltammograms in the solution of 4.0 mmol L^{-1} $K_3[Fe(CN)_6]$ in 0.1 mol L^{-1} KCl at scan rates of 10, 20, 40, 70, 100, 150, 200 and 300 mV s^{-1}; (B) plot of peak currents versus scan rate; (C) plot of peak currents versus square root of scan rate*

Electrochemistry of UA on LZH-SDS-PRO/MWCNT paste electrode

The square wave voltammetry (SWV) measurements were carried out to compare electroanalytical performance of the non-modified MWCNT and LZH-SDS-PRO/MWCNT paste electrodes. As illustrated in Figure 6, the peak current of UA oxidation at the non-modified MWCNT is observed at 5.613 µA.

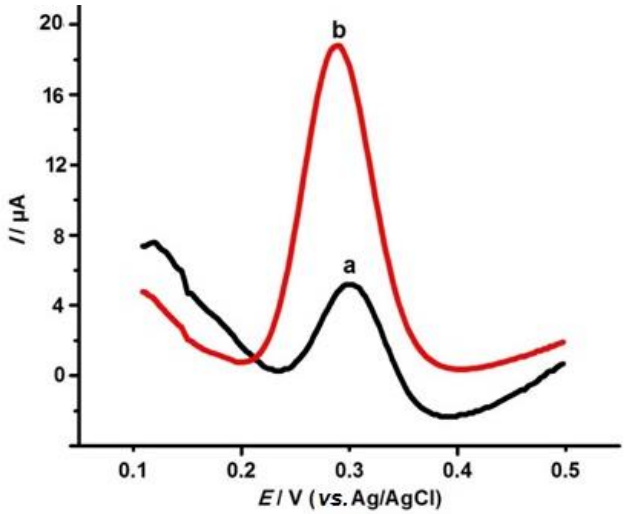

Figure 6. *SW Voltammograms in the solution of 0.1 mmol L^{-1} UA in 0.1 mol L^{-1} PBS at pH 6.4 using: (a) non-modified MWCNT and (b) LZH-SDS-PRO/MWCNT*

The oxidation peak current of LZH-SDS-PRO/MWCNT, however, is dramatically improved by the factor of 3 to 18.16 µA. Except for the effect of increased surface area, this might be due to the excellent electrical conductivity of LZH-SDS-PRO/MWCNT that can act as an effective electrons promoter during the electrochemical reaction. Hence, the addition of LZH-SDS-PRO into MWCNT has enhanced the electrode performance for the detection of UA.

Scheme 1 illustrates the proposed mechanism for the oxidation reaction of UA at the LZH-SDS--PRO/MWCNT paste electrode. By UA oxidation, imine alcohol is produced from UA by donating two protons and electrons, while two moles of propoxur at the electrode surface accept those protons and electrons to produce *o*-isopropoxyphenol [31,32].

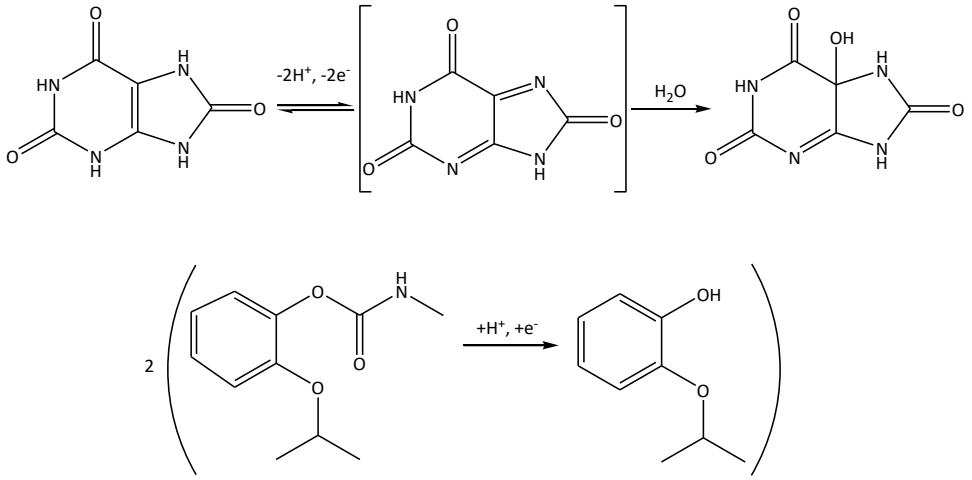

Scheme 1. *Probable mechanism of oxidation reaction of UA at LZH-SDS-PRO/MWCNT paste electrode*

The effect of pH

Figure 7 shows how pH values between 6.0 and 8.0 of 0.1 mol L^{-1} PBS affect the oxidation peak currents of 0.1 mmol L^{-1} UA at LZH-SDS-PRO/MWCNT paste electrode since PBS was optimized at the pH scale of 6.2 to 8.0 [33]. The oxidation peak current of UA increased with increasing the pH value from 6.0, reached a maximum point at pH 6.4, and then decreased with further pH increasing. Therefore, throughout the work for UA determination, the optimum pH was set at 6.4. It is clearly seen from Figure 7 that the peak potential shifted negatively with pH increase, proving thus the involvement of protons in the oxidation of UA.

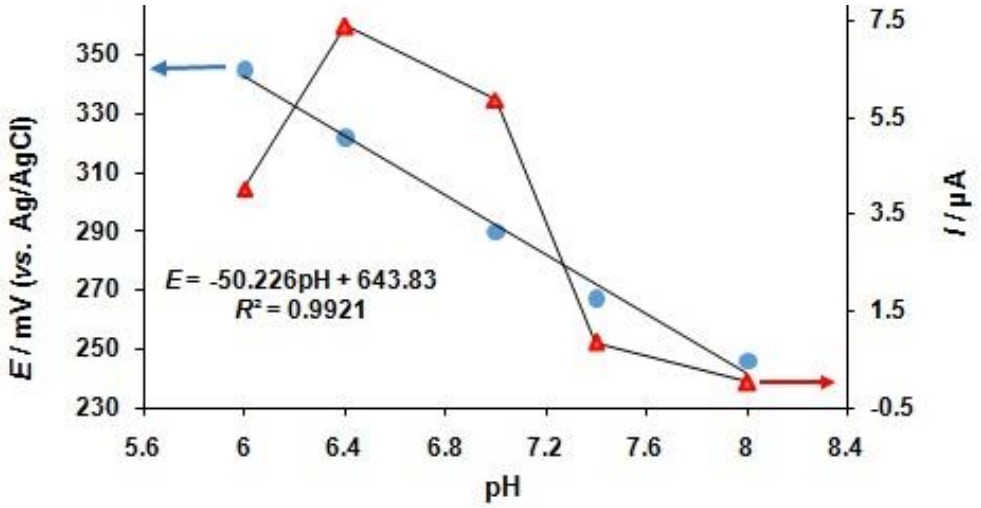

Figure 7. *Plot of oxidation peak current (I) and oxidation potential (E) vs. pH of 0.1 mol L^{-1} PBS containing 0.1 mmol L^{-1} UA at LZH-SDS-PRO/MWCNT paste electrode*

The relationship between pH and peak potential (E) of UA can be expressed as: E = -50.226 pH + + 643.83 (R^2 = 0.9921), suggesting the equal number of electrons and protons involved in the electrochemical oxidation of UA at LZH-SDS-PRO/MWCNT. This conclusion is based on the obtained slope of 50.226 mV pH^{-1}, close to the Nernst value of 59 mV pH^{-1} [34].

Calibration curve and limit of detection

In order to study the relationship between the concentration of UA and oxidation peak current (I) on the LZH-SDS-PRO/MWCNT paste electrode, a series of UA solutions was prepared, containing 7.0 µmol L^{-1} to 0.7 mmol L^{-1}. As shown in Figure 8A, I increased linearly as UA concentrations were increased. The plot of I *vs*. [UA] showed a linear relationship with the following linear regression equation: I = 0.058 c_{UA} – 1.417 (R^2 = 0.9920) and the limit of detection (LOD) was found to be 4.28 µmol L^{-1}. LOD was determined using eq. (2):

$$LOD = 3\sigma / m \quad (2)$$

where m = slope of the calibration curve and σ = relative standard deviation of its intercept.

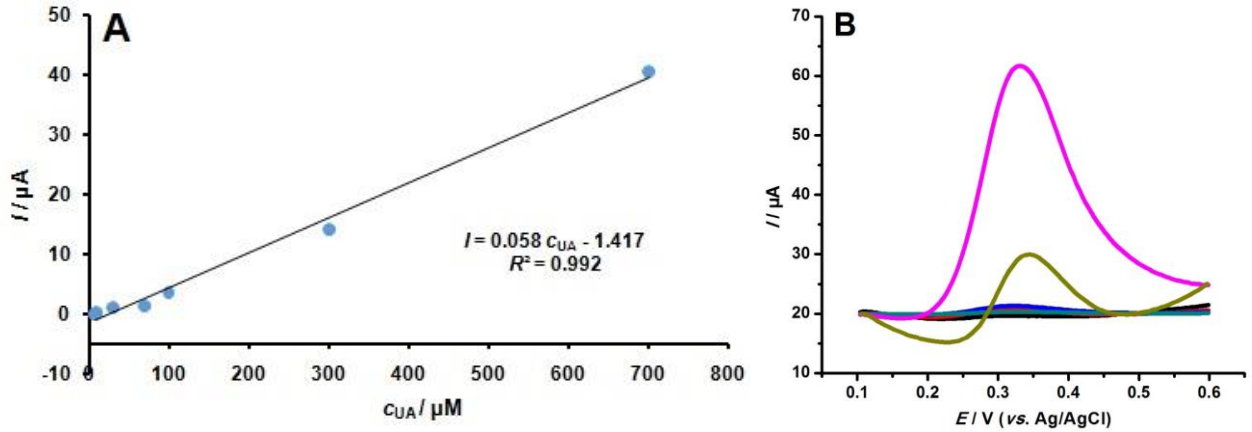

Figure 8. *(A) Linear plot of I vs. c_{UA} and (B) SWVs at different concentrations (7, 10, 30, 70, 100, 300 and 700 µM) of UA in 0.1 mol L^{-1} PBS (pH 6.4)*

The high sensitivity of the LZH-SDS-PRO/MWCNT paste electrode compared to those obtained for several other electrodes by different electroanalytical methods is presented in Table 1. The obtained results proved that the suggested sensor can be used for the determination of UA in environmental and even biological analytes.

Table 1. *Comparison of analytical properties of different fabricated electrodes for the determination of UA*

Electrode materials	Method	Linear range of concentration, µmol L^{-1}	LOD, µmol L^{-1}	Ref.
DMF / SPCE	DPV	100.0 – 500.0	0.19	[35]
Poly(Isoniazid) / CPE	CV	10.0 – 1000.0	1.173	[36]
PEDOT / GCE	CV	6.0 – 100.0	7.0	[37]
MWCNT-PEDOT / GCE	DPV	10.0 – 250.0	10.0	[38]
GF / $NiCo_2O_4$	SWV	10.0 – 26.0	0.2	[39]
MWCNT / GCE	SWV	10.0 – 200.0	1.0	[40]
LZH-SDS-PRO / MWCNT / CPE	SWV	7.0 – 700.0	4.28	This work

Selectivity, stability, reproducibility and repeatability of LZH-SDS-PRO/MWCNT paste electrode

The selectivity of the LZH-SDS-PRO/MWCNT paste electrode was tested by evaluating differrences in the oxidation peak current value of 0.1 mmol L^{-1} UA in 0.1 mol L^{-1} PBS (pH 6.4) in the presence of possible coexisting interfering species such as *D*-glucose, *L*-fructose, and Na^+, Mg^{2+}, Ca^{2+}, Cl^-, SO_4^{2-}

and NO_3^- ions. As illustrated in Figure 9, LZH-SDS-PRO/MWCNT paste electrode has the anti-interference ability in the presence of 10- and 50- fold higher concentrations of interfering species with the relative error of less than ± 10 %.

The stability of the fabricated paste electrode was recorded towards 0.1 mmol L^{-1} UA in 0.1 mol L^{-1} PBS (pH 6.4) within 14 days and the results were retained about 90 % from the initial response, indicating high stability of electrode over a long period.

The reproducibility of the fabricated paste electrode was conducted using five individual electrodes prepared by the same procedure. The relative standard deviation (RSD) of these electrodes was 3.19 %. Moreover, the RSD value of 4.73 % obtained after 10 successive measurements with similarly fabricated electrodes suggested that LZH-SDS-PRO/MWCNT paste electrode can be used repeatedly for the determination of UA.

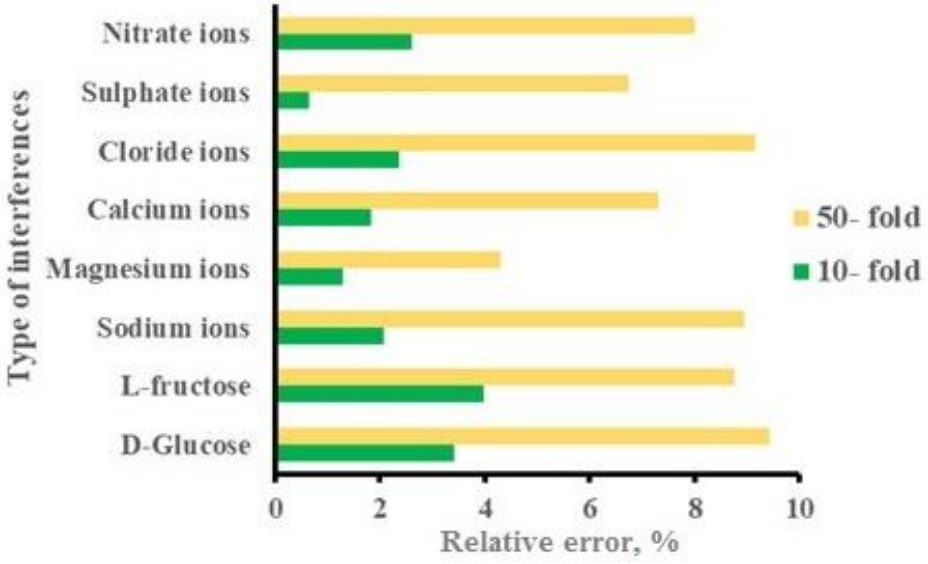

Figure 9. *Interference analysis of 0.1 mmol L^{-1} UA at LZH-SDS-PRO/MWCNT paste electrode*

Real samples analysis

The validity of the results obtained using the LZH-SDS-PRO/MWCNT paste electrode was studied by determining the concentration of UA in the urine sample *via the* standard addition method. The urine sample was directly diluted 30 times in 0.1 mol L^{-1} PBS (pH 6.4) without pre-treatment. Then, known concentrations of UA were spiked into the urine sample to study electrode recoveries. As a result, LZH-SDS-PRO/MWCNT paste electrode exhibited good recoveries, as summarized in Table 2.

Table 2. *Determination of UA in urine sample using LZH-SDS-PRO/MWCNT paste electrode (n = 3)*

Sample	c_{UA} / µmol L^{-1}			Recovery, %	RSD, %
	Determined	Spiked	Found		
Urine	140.3	100	243.8	101.5	3.81
		200	337.3	99.1	2.94
		300	445.7	101.2	3.72

Conclusions

In this experiment, a simple, highly sensitive, and cost-effective sensing material was proposed for the determination of UA with low LOD. These beneficial sensing electrode properties were realized through a combination of unique properties of LZH-SDS-PRO nanomaterial and MWCNT.

The prepared nanocomposite electrode exhibited significant electrocatalytic activity toward UA oxidation with satisfactory results of selectivity, stability and reproducibility, suggesting that LZH-SDS-PRO/MWCNT paste electrode is an attractive candidate for practical applications.

Acknowledgment: *The authors would like to extend their gratitude to the Research Management and Innovation Centre (RMIC), Sultan Idris Education University (UPSI) for the University Research Grants (GPU-F: 2019-0218-103-01) that helped fund the research.*

References

[1] Y. V. M. Reddy, B. Sravani, S. Agarwal, V. K. Gupta, G. Madhavi, *Journal of Electroanalytical Chemistry* **820** (2018) 168-175. https://doi.org/10.1016/j.jelechem.2018.04.059
[2] L. Carvalho, J. Lopes, G. H. Kaihami, R. P. Silva, A. Brunicardoso, R. L. Baldini, F. C. Meotti, *Redox Biology* **16** (2018) 179-188. https://doi.org/10.1016/j.redox.2018.02.020
[3] L. Rana, R. Gupta, M. Tomar, V. Gupta, *Sensors and Actuators B* **261** (2018) 169-177. https://doi.org/10.1016/j.snb.2018.01.122
[4] J. Jiang, X. Du, *Nanoscale* **6** (2014) 11303-11309. https://doi.org/10.1039/C4NR01774A
[5] R. Ahmad, N. Tripathy, M. S. Ahn, Y. B. Hahn, *Scientific Reports* **7** (2017) 46475. https://doi.org/10.1038/srep46475
[6] L. Zhao, J. Blackburn, C. L. Brosseau, *Analytical Chemistry* **87** (2015) 441-447. https://doi.org/10.1021/ac503967s
[7] J. Wang, M. P. Chatrathi, B. Tian, R. Polsky, *Analytical Chemistry* **72** (2000) 2514-2518. https://doi.org/10.1021/ac991489l
[8] R. Sakuma, T. Nishina, M. Kitamura, *Clinical Chemistry* **33** (1987) 1427-1430. https://doi.org/10.1093/clinchem/33.8.1427
[9] M. Czauderna, J. Kowalczyk, *Journal of Chromatography B: Biomedical Sciences and Applications* **744** (2000) 129-138. https://doi.org/10.1016/S0378-4347(00)00239-5
[10] J. Yu, S. Wang, L. Ge, S. Ge, *Biosensensors and Bioelectronics* **26** (2011) 3284-3289. https://doi.org/10.1016/j.bios.2010.12.044
[11] J. C. Fanguy, C. S. Henry, *Electrophoresis* **23** (2002) 767-773. https://doi.org/10.1002/1522-2683(200203)23:5%3C767::AID-ELPS767%3E3.0.CO;2-8
[12] J. Tang, S. Jiang, Y. Liu, S. Zheng, L. Bai, J. Guo, J. Wang, *Microchimica Acta* **185** (2018) 486. https://doi.org/10.1007/s00604-018-3025-x
[13] B. Han, M. Pan, X. Liu, J. Liu, T. Cui, Q. Chen, *Materials (Basel)* **12** (2019) 214. https://doi.org/10.3390/ma12020214
[14] B. Demirkan, S. Bozkurt, A. Şavk, K. Cellat, F. Gulbagca, M. S. Nas, M. H. Alma, H. Sen, *Scientific Reports* **9** (2019) 12258. https://doi.org/10.1038/s41598-019-48802-0
[15] H. Rajabi, M. Noroozifar, N. Sabbaghi, *Journal of Materials & Applied Science* **1(1)** (2017) 1002. https://www.jscimedcentral.com/Materials/Articles/materials-1-1002.pdf
[16] S. Z. Mohammadi, H. Beitollahi, Z. Dehghan, R. Hosseinzadeh, *Applied Organometallic Chemistry* **32** (2018) e4551. https://doi.org/10.1002/aoc.4551
[17] S. Iijima, *Nature* **354** (1991) 56-58. https://doi.org/10.1038/354056a0
[18] A. Cernat, M. Tertis, R. Sandulescu, F. Bedioui, A. Cristea, C. Cristea, *Analytica Chimica Acta* **886** (2015) 16-28. https://doi.org/10.1016/j.aca.2015.05.044
[19] J. H. Zagal, S. Griveau, M. Santander Nelli, S. G. Granados, F. Bedioui, *Journal of Porphyrins and Phthalocyanines* **16** (2012) 713-740. https://doi.org/10.1142/S1088424612300054
[20] S. Wang, J. Yang, X. Zhou, J. Xie, L. Ma, B. J. Huang, *Journal of Electroanalytical Chemistry* **722** (2014) 141-147. https://doi.org/10.1016/j.jelechem.2014.04.001
[21] J. Simon, E. Flahaut, M. Golzio, *Materials (Basel)* **12** (2019) 624-644. https://doi.org/10.3390/molecules25245827

[22] N. A. Azis, I. M. Isa, N. Hashim, M. S. Ahmad, S. N. A. M. Yazid, M. I. Saidin, M. S. Suyanta, R. Zainul, A. Ulianas, S. Mukdasai, *International Journal of Electrochemical Sci*ence **14** (2019) 10607-10621. https://doi.org/10.20964/2019.11.46
[23] M. S. Ahmad, I. M. Isa, N. Hashim, M. S. Rosmi, S. Mustafar, *International Journal of Electrochemical Sci*ence **13** (2018) 373-383. https://doi.org/10.20964/2018.01.31
[24] M. S. Ahmad, I. M. Isa, N. Hashim, M. S. Suyanta, M. I. Saidin, *Journal of Solid State Electrochemistry* **22** (2018) 2691-2701. https://doi.org/10.1007/s10008-018-3979-y
[25] M. S. Ahmad, I. M. Isa, N. Hashim, M. I. Saidin, M. S. Suyanta, R. Zainul, A. Ulianas, S. Mukdasai, *International Journal of Electrochemical Sci*ence **14** (2019) 9080-9091. https://doi.org/10.20964/2019.09.54
[26] Z. Muda, N. Hashim, I. M. Isa, N. M. Ali, S. A. Bakar, M. Mamat, M. Z. Hussein, N. A. Bakar, W. R. W. Mahamod, *International Fundamentum Science Symposium*, *IOP Conferece Series: Materials Science and Engineering* **440** (2018) 012003. http://dx.doi.org/10.1088/1757-899X/440/1/012003
[27] Q. Yan, N. Zhi, L. Yang, G. Xu, Q. Feng, Q. Zhang, S. Sun*, Scientific Reports* **10** (2020) 10607. https://doi.org/10.1038/s41598-020-67394-8
[28] A. Xu, Y. Weng, R. Zhao, *Materials* **13** (2020) 1179-1198. https://doi.org/10.3390/ma13051179
[29] C. O. Chikere, N. H. Faisal, P. Kong Thoo Lin, C. Fernandez, *Nanomaterials* **10** (2020) 537-562. https://doi.org/10.3390/nano10030537
[30] W. Zhang, L. Liu, Y. Li, D. Wang, H. Ma, H. Ren, Y. Shi, Y. Han, B.C. Ye, *Biosensors and Bioelectronics* **121** (2018) 96-103. https://doi.org/10.1016/j.bios.2018.08.043
[31] M. F. Simoyi, E. Falkenstein, K. V. Dyke, K. P. Blemings, H. Klandorf, Comparative Biochemistry and Physiology Part B: Biochemistry and Molecular Biology **135** (2003) 325-335. https://doi.org/10.1016/s1096-4959(03)00086-1
[32] P. Kovacic, R. Somanathan, *Propoxur: A Novel Mechanism for Insecticidal Action and Toxicity. Reviews of Environmental Contamination and Toxicology*, Springer, Boston, United State, 2012, p. 141. https://doi.org/10.1007/978-1-4614-3137-4_4
[33] Z. Hua, Q. Qin, X. Bai, C. Wang, X. Huang, *Sensors and Actuators B* **220** (2015) 1169-1177. https://doi.org/10.1016/j.snb.2015.06.108
[34] J. Ning, Q. He, X. Luo, M. Wang, D. Liu, J. Wang, G. Li, J. Liu, *Catalysts* **8** (2018) 407. https://doi.org/10.3390/catal8100407
[35] M. Metto, S. Eramias, B. Gelagay, A. P. Washe, *International Journal of Electrochemistry* **2019** (2019) 1-8. https://doi.org/10.1155/2019/6318515
[36] M. P. Deepak, G. P. Mamatha, B. S. Sherigara, *International Journal of Pharmaceutical Chemistry* **4** (2014) 122-129. **ISSN:** 2249-734X
[37] M. Motshakeri, J. Travas Sejdic, A. R. J. Phillips, P. A. Kilmartin, *Electrochimica Acta* **265** (2018) 184-193. https://doi.org/10.1016/j.electacta.2018.01.147
[38] K. C. Lin, T. H. Tsai, S. M. Chen, *Biosensors and Bioelectronics* **26** (2010) 608-614. https://doi.org/10.1016/j.bios.2010.07.019
[39] Y. Peng, D. Zhang, C. Zhang, *Analytical Methods* **6** (2014) 8965-8972. https://doi.org/10.1039/C4AY01029A
[40] H. Q. Bi, Y. H. Li, S. F. Liu, P. Z. Guo, Z. B. Wei, C. X. Lv, J. Z. Zhang, X. S. Zhao, *Sensors and Actuators B* **171** (2012) 1132-1140. https://doi.org/10.1016/j.snb.2012.06.044